MD Simulations of the Binding of Alcohols and Diols by a Calixarene in Water: Connections between Microscopic and Macroscopic Properties

A. Ghoufi, J. P. Morel, N. Morel-Desrosiers, and P. Malfreyt*

Laboratoire de Thermodynamique des Solutions et des Polymères, UMR CNRS 6003, Université Blaise Pascal (Clermont-Ferrand II), 24 avenue des Landais, 63177 Aubière Cedex, France

Received: August 31, 2005; In Final Form: October 11, 2005

We report results of molecular dynamics (MD) simulations of the complexes of *p*-sulfonatocalix[4]arene with linear alcohols from ethanol to heptanol in water at 25 °C. We show that these complexes are of the inclusion type and are governed by van der Waals interactions between the calixarene cavity and the inserted alkyl chain of the alcohol. We establish a correlation between the experimental $\Delta_r H°$ values and the number of atoms inserted into the calixarene cavity. We also focus on the desolvation of the host and guest to establish the importance, at the enthalpic level, of the formation of hydrogen bond bridges between the calixarene and the alcohol molecule. The fact that methanol is not complexed by *p*-sulfonatocalix[4]arene is explained by calculating the cost of the desolvation of the guest upon complexation. We complete this study by modeling the complexes formed with 1,4-butanediol and 1,5-pentanediol. To explain the difference between the thermodynamic properties for the binding of 1,4-butanediol and butanol, we examine the insertion rate and the solvation of each hydroxy group. We show a specific behavior of one of the two hydroxy groups at the structural and energetic levels.

Introduction

The *p*-sulfonatocalixarenes, because they are water-soluble, constitute a particularly interesting class of synthetic hosts for bioorganic and biomimetic chemistry.[1] Within this family, *p*-sulfonatocalix[4]arene, shown in Figure 1a and represented by **1** throughout this paper, is a remarkable ligand that can complex a variety of organic compounds and inorganic cations in water.[1−3,5,6] Depending on the guest, different types of weak interactions may be involved (ionic, hydrophobic, van der Waals, $\pi-\pi$, cation$-\pi$, hydrogen bonding, ...). To understand how this host can recognize biomolecules, it is essential to identify first the factors that govern the formation of supramolecular complexes with a simple model guest bearing different functional groups.

A complete thermodynamic characterization of the binding process, which includes the enthalpy and entropy of association, is one of the key elements in identifying the stabilizing factors and in understanding how the host and guest assemble. During the past few years, we used microcalorimetry, which is a powerful tool for measuring the thermodynamic parameters that characterize interacting molecules, to study the binding of **1** with the basic amino acids lysine and ariginine[4] and also with dipeptides and tripeptides bearing lysine or arginine residues.[5] We also used it to study the binding of **1** with alkylammonium cations,[3,6] alkanols,[6] and divalent and trivalent inorganic cations.[3] The microcalorimetric results clearly showed that these species bind in very different modes: in fact, for all the organic guests, the binding process is enthalpy-driven ($\Delta_r H° \ll 0$ and $T\Delta_r S° <$ 0 or > 0) whereas it is entropy-driven for the inorganic cations ($\Delta_r H° > 0$ and $T\Delta_r S° \gg 0$). The binding of **1** with an organic guest is enthalpy-driven because the guest is partly or completely included in the host cavity (see Figure 2). Upon inclusion, the host and guest lose most of their degrees of freedom ($\Delta S < 0$)

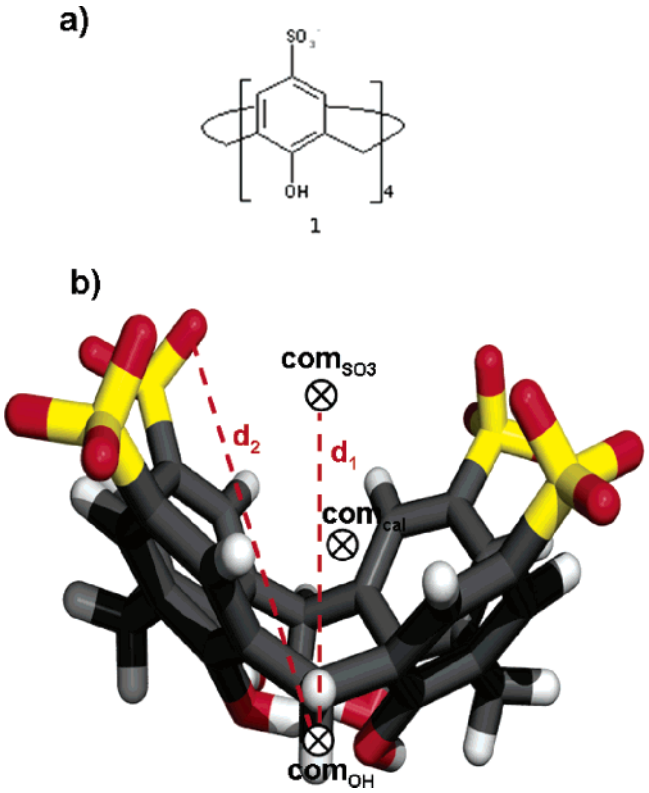

Figure 1. (a) *p*-Sulfonatocalix[4]arene and (b) schematic representation of the *p*-sulfonatocalix[4]arene with the location of typical points. The symbol ⊗ represents the position of the peculiar center of mass. com_{cal} refers to the com of the calixarene and com_{SO_3} to the com of the four sulfonate groups of the upper rim and com_{OH} to the com of the four hydroxy groups of the lower rim. d_1 and d_2 are specific distances as indicated in the scheme.

* To whom correspondence should be addressed. E-mail: Patrice.MALFREYT@univ-bpclermont.fr.

10.1021/jp054925i CCC: $30.25
Published on Web 11/19/2005

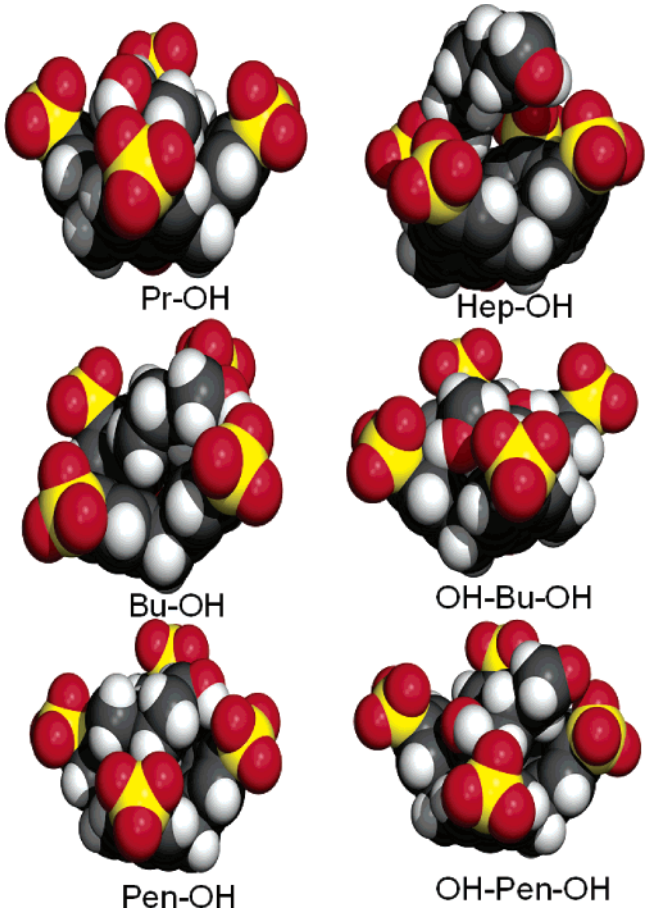

Figure 2. Snapshots of complexes of *p*-sulfonatocalix[4]arene with alcohols and diols.

and part of their solvation ($\Delta S > 0$); as a result, the binding process is controlled by van der Waals interactions that occur between the host and guest maintained at a short distance ($\Delta H < 0$). At the opposite, the association of **1** with a divalent or trivalent inorganic cation is entropy-driven because the guest remains outside the cavity and forms purely ionic binding with the sulfonate groups of **1**. As classically observed for the formation of various ion pairs,[7] the process is characterized by $\Delta_r H° > 0$ and $T\Delta_r S° \gg 0$ due to the partial desolvation of the charged species.

In addition to the thermodynamic characterization of the binding process, we studied the molecular structures of the complexes using MD simulations.[8−10] First, we showed that the complexation of **1** with lanthanide cations involves the formation of external complexes, with the cation located slightly above the sulfonate groups.[8] We established the desolvation of the second hydration shell of the cation and showed that the complex is of the outer-sphere type (solvent-shared ion pair). The insertion of tetraalkylammonium cations into the calixarene cavity was also deeply investigated.[9,10] We established a correlation between the experimental $\Delta_r H°$ and the number of methylene groups inserted into the cavity and explained the specific behavior of Et_4N^+ by the largest number of inserted atoms. Last, we developed perturbation algorithms to calculate the difference between the Gibbs free energies of association of **1** with Me_4N^+ and $MeNH_3^+$ in acidic aqueous solution.[10]

In the present paper, we perform molecular simulations of the binding of linear alcohols and diols by **1** in water at 25 °C. We aim to give a molecular description of these complexes in line with the microcalorimetry results.[6] Throughout this paper, we do not intend to calculate differences of Gibbs free energies of **1** with different alcohols. This kind of calculation has been already successfully carried out for the complexation of **1** with alkylammonium cations[10] and has shown the reliability of the potential and methodology used. The structural and energetic characterization of the complexes formed with alcohols and diols requires us to calculate some energy contributions between the host and guest and to analyze the desolvation of the species. The potential model and the appropriate methodology for the simulation of complexes of **1** with linear alcohols from ethanol to heptanol and with 1,4-butanediol and 1,5-pentanediol in water are presented. The effects of the presence of hydroxy groups in the alcohol and diol molecules are analyzed as a function of the alkyl chain length and are underscored throughout comparisons with previous simulations.[8,9]

2. Simulation

2.1. Potential Models. The *p*-sulfonatocalix[4]arene molecule is modeled using the all-atom (AA) version of the Cornell force field AMBER.[11] The general potential function is of the form

$$U = \sum_{\text{bonds}} k_b(r - r_o)^2 + \sum_{\text{angles}} k_\theta(\theta - \theta_o)^2 + \sum_{\text{dihedrals}} k_\phi[1 + \cos(l\phi + \delta)] + \sum_{i=1}^{N-1}\sum_{j=i+1}^{N}\left\{4\epsilon_{ij}\left[\left(\frac{\sigma_{ij}}{r_{ij}}\right)^{12} - \left(\frac{\sigma_{ij}}{r_{ij}}\right)^{6}\right] + \sum_{l}^{\infty}{}' \frac{q_i q_j}{|\mathbf{r_{ij}} + \mathbf{n}L|}\right\} \quad (1)$$

where k_b, k_θ, and k_ϕ are the force constants for deformation of bonds, angles, and dihedrals, respectively. The equilibrium values of bond distances and valence angles correspond to r_o and θ_o, respectively. In the dihedral angle term, l is the periodicity and δ is the phase factor. The last term in eq 1 corresponds to the electrostatic energy of the system where $\mathbf{r_{ij}} = \mathbf{r_i} - \mathbf{r_j}$ and $\mathbf{r_i}$ represents the position of the point charge q_i. The prime just after the summation term indicates that the sum is performed over all periodic images, $\mathbf{n} = (n_x L_x, n_y L_y, n_z L_z)$ with n_x, n_y, and n_z integers, and over atoms j, except $j = i$ if $\mathbf{n} = 0$. The C−H and O−H covalent bonds are kept of fixed length by use of the SHAKE algorithm,[12] and the aromatic rings are kept planar using six improper torsional potentials. The intermolecular and intramolecular interactions consist of a van der Waals repulsion-dispersion term calculated using the Lennard-Jones (6-12) potential, represented by the penultimate term in eq 1. In the AMBER force field, the nonbonded interactions between atoms separated by exactly three bonds (1−4 van der Waals interactions) are reduced by a factor of 0.5.[11] The parameters of the sulfonate groups are taken in ref 13. As concerns the description of the alcohol molecules, we change the torsional expression shown in eq 1 by a 3-fold Fourier series and scale down the intramolecular 1,4 interactions by 5 as proposed in the original paper.[14] The Lennard-Jones potential parameters for the interactions between unlike atoms are calculated by using the Lorentz−Berthelot mixing rules (quadratic and arithmetic rules for the ϵ_{ij} and σ_{ij} parameters, respectively). The water molecules are represented with the TIP3P model.[15] The electrostatics interactions are calculated using the Ewald sum method[16,17] with the different contributions

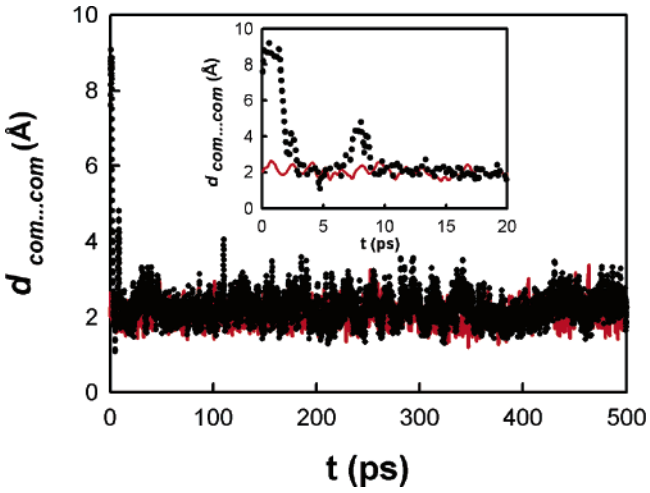

Figure 3. Trajectories of the distance between the calixarene com and propanol com during the equilibration phase in two limit cases. The black dotted line corresponds to the trajectory of the propanol initially located above the sulfonate groups whereas the red solid line represents the trajectory of the propanol initially inserted into the calixarene cavity. The inset shows an enlargement of these trajectories over the first 20 ps.

given by the following formula

$$U_{\text{elec}} = \frac{1}{8\pi\epsilon_o}\sum_i\sum_a\sum_j\sum_{b\neq a}\left(\sum_{|n|=0}^{\infty}{}' \frac{q_{ia}q_{jb}}{|r_{iajb}+n|}\,erfc(\alpha|r_{iajb}+n|)\right) + \frac{1}{2V\epsilon_o}\sum_{k\neq 0}\frac{1}{k^2}\exp\left(-\frac{k^2}{4\alpha^2}\right)|\sum_i\sum_a q_{ia}\exp(ik\cdot r_{ia})|^2 - \frac{1}{8\pi\epsilon_o}\sum_i\sum_a\sum_{b\neq a}\frac{q_{ia}q_{ib}}{r_{iaib}}erf(\alpha r_{iaib}) - \frac{\alpha}{4\pi^{3/2}\epsilon_o}\sum_i\sum_a {q_{ia}}^2 \quad (2)$$

where n is the lattice vector of the periodic array of MD cell images. a and b denote atoms of molecules i and j, respectively. In the first term of eq 2, when $i = j$, the summation discounts any excluded atoms b of atom a. Remember that the excluded atoms b of atom a are atoms that are linked through a bond, angle, or torsion to atom a. The third term in eq 2 indicates that the summations run over only the excluded atoms b of atom a in the molecule i. r_{iajb} is the distance between the atoms a and b belonging to the two different molecules i and j. q_{ia} and q_{ib} represent the charges on atoms a and b, respectively.

2.2. Computational Methodology. The system consists of one *p*-sulfonatocalix[4]arene molecule with an alcohol molecule and 900 water molecules. Four Na^+ cations are added to ensure the electroneutrality in the simulation box. To simulate the free alcohols in solution, we use a simulation box of 30 Å with 900 water molecules. In acidic solutions at pH 2, all the phenolic hydroxy groups are protonated according to the pK_a values.[18−20] The sodium cation is located in such a way that the Na^+...Na^+ and Na^+...calixarene distances are larger than the cutoff radius. To be sure that the equilibrium conformation of the complex does not depend on the initial configuration, we have tested two starting conformations differing in the distance between the centers of mass of **1** and alcohol. Two situations are attempted: insertion of the guest into the calixarene cavity and location of the guest above the sulfonate groups. Figure 3 shows the trajectories of the distance between the centers of mass of calixarene and an alcohol molecule in the two limit initial positions. We check that the two trajectories calculated during the equilibration phase converge within a time of 20 ps to the same value, which is typical of that calculated for an inclusion complex.

The periodic boundary conditions are applied in three dimensions. The long-range electrostatic interactions are evaluated by the Ewald summation technique. The parameters of this method are $\alpha = 0.2651$ (convergence parameter) within a relative error of 10^{-6} and $k_{max} = \{8 \times 8 \times 8\}$ (the reciprocal space vetors). The equations of motions are integrated using the Verlet Leapfrog algorithm scheme in the *NpT* ensemble ($p = 1$ atm and $T = 298$ K) with 2 fs as the time step. We apply the multiple time step algorithm[21] in which two steps of different lengths are used to integrate the equation of motions. With this algorithm, the CPU time is decreased by a factor varying from 3 to 8. The simulations are performed in the *NpT* ensemble using the Berendsen algorithm[22] with coupling constants 0.1 ps (temperature) and 0.5 ps (pressure). The Verlet list sphere radius is fixed to 14 Å. A typical run consisted of 500 ps of equilibration followed by a production phase of an additional 1 ns. The structural and thermodynamic properties are calculated over 50 000 configurations saved during the acquisition phase. The configurations are generated using the parallel version of the DL_POLY_MD package[25] by using up to 16 processors at a time.

The atomic charges are fitted to reproduce the molecular electrostatic potential created around each molecule at the HF level with the 6-31G* basis for the calixarene anion and 6-31G** basis for the alcohol molecules. We use the CHELPG[23] procedure as a grid-based method. The quantum ab initio calculations are carried out using the GAMESS package.[24] The fact that the Amber force field[11] relies on the use of the 6-31G* basis leads us to compare the two bases on the charges of the alcohol molecules. We do not observe any significant changes between the two bases. The maximum deviation between the set of charges is of the order of 0.07 e.

3. Results and Discussions

3.1. Binding with Alcohols. 3.1.1. Structures and Energetics. We have shown in previous papers that the cavity of **1** can be represented by a sphere whose radius is approximately equal to 5 Å. This radius value has been calculated from the definition of the radius of gyration,[8] and the shape of the calixarene cavity has been established from the calculation of the asphericity coefficient.[8] The use of the radius of gyration has proved to be efficient for complexes involving tetraalkylammonium cations. However, for alcohol guests, we need to take into account additional typical distances (Figure 1b) to be sure to carefully sample the region slightly above the sulfonate groups. Throughout this paper, we symbolize the center of mass (com) of the four hydroxy groups of the lower rim by com_{OH}, the com of the four sulfonate groups of the upper rim by com_{SO_3}, and we define d_1 as the distance between com_{OH} and com_{SO_3} and d_2 as the largest distance between the oxygen atoms of the sulfonate groups and com_{OH}. As concerns the complexes of **1** with alcohols and diols, d_1 is equal to 6 Å and d_2 to 7.5 Å.

The distance between the centers of mass (com's) of the calixarene and alcohol is represented in part a of Figure 4 for ethanol (Et-OH) to heptanol (Hep-OH). We observe that this distance increases from 2.0 ± 0.3 Å to 4.2 ± 0.7 Å and varies with the length of the alkyl chain. The fact that this distance is always smaller than the radius of gyration of the cavity of **1**

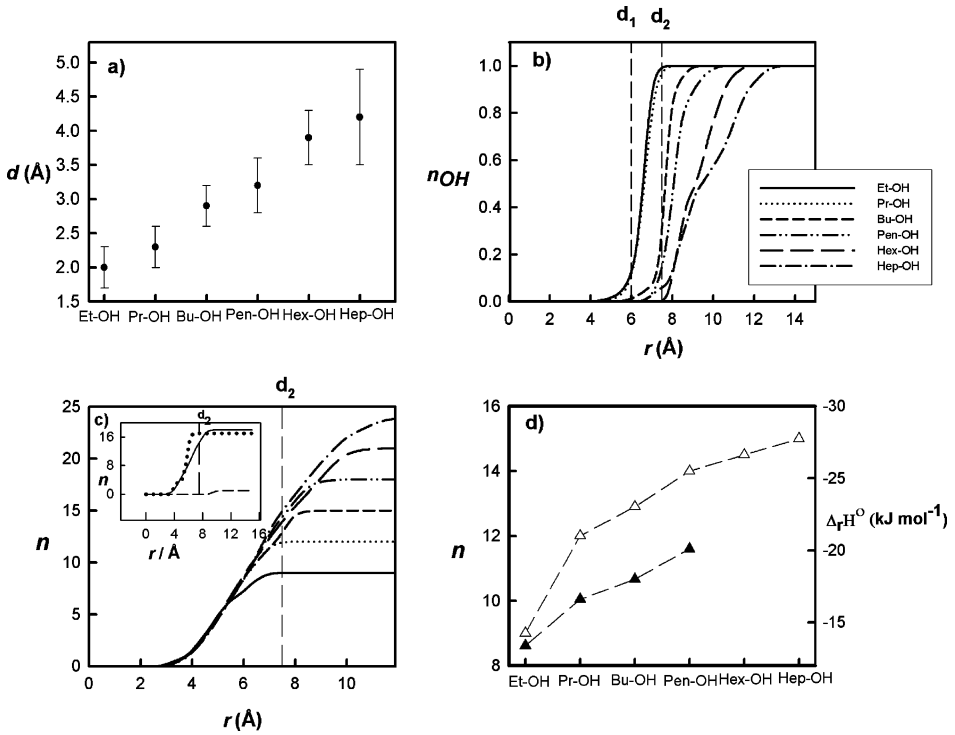

Figure 4. (a) Average distances between the com of **1** and the com of the alcohol molecules; (b) integrations of the distribution of the distance from the hydroxy group of the alcohol to com_{OH}; (c) integrations of the distributions of the distance from each atom of the alkyl chain of the alcohol to com_{OH} with the same legend as that used for b. The inset shows these integration curves for the complexes with Me_4N^+ (dotted curve), La^{3+} (dashed curve), and Pen-OH (solid curve); (d) $\Delta_r H°$ (▲, right axis) and number of atoms (△, left axis) inserted into the host cavity upon the complexation of alcohols.

indicates that the alkyl chain is partly inserted into the cavity of the macrocyclic host (Figure 2). To describe more thoroughly the insertion process, we have plotted in Figure 4b the integration of the distribution of the distance between com_{OH} and the hydroxy group of the alcohol. This figure shows that the hydroxy group of the alcohol molecule moves away from the upper rim as the alkyl chain length of the guest increases. The OH group of Et-OH and Pr-OH can be considered as totally inserted into the lipophilic cavity of **1** whereas it is only partially inserted for alcohols with longer alkyl chains. In fact, from Hep-OH, the integration curves are shifted to larger distances, showing that the OH group is located above the sulfonate groups with a distance greater than d_2. In contrast, the integration curves of the distributions of the distances between each atom of the alkyl chain and com_{OH} highlight deeper insertions for the alkyl groups than for the OH group. The inset in Figure 4c shows a comparison over the integration curves for the Me_4N^+, Pen-OH, and La^{3+} guests. More generally, we show that the insertion is deeper for a tetraalkylammonium cation than for an alcohol having approximately the same number of atoms. For comparison, the external complex formed with an inorganic cation such as La^{3+} is clearly identified by a zero distribution inside the cavity of the macrocycle. For the alcohols, we have calculated the number of inserted atoms at the limit separation distance d_2 of 7.5 Å: it increases from 9 for Et-OH to 14.4 for Hep-OH. This number of inserted atoms and the $\Delta_r H°$ experimental values are plotted as a function of the alkyl chain length in part d of Figure 4. A correlation between the enthalpy changes and the number of groups inserted inside the cavity is observed. A similar correlation was previously observed for the binding of tetraalkylammonium cations. Figure 4d also shows that the number of inserted atoms does not significantly increase from Pen-OH, indicating an optimal fit of the cavity by the pentyl group.

TABLE 1: Dispersive and Repulsive Parts of the Lennard-Jones Potential and Electrostatic Part for the Calixarene−Alcohol Interaction Energy[a]

	$E_{dispersive}$ (kJ mol^{-1})	$E_{repulsive}$ (kJ mol^{-1})	$E_{electrostatic}$ (kJ mol^{-1})
Et-OH	-65.2_{12}	30.5_{19}	-3.6_4
Pr-OH	-76.9_{11}	35.9_{11}	-5.4_{15}
Bu-OH	-91.9_{13}	50.6_{16}	-6.4_{21}
Pen-OH	-98.2_{12}	52.2_{11}	-6.9_{28}
Hex-OH	-101.5_{14}	55.2_{17}	-7.4_{13}
Hep-OH	-104.9_{18}	55.6_{11}	-6.5_{22}
La^{3+}	-12.1_{18}	64.1_{11}	-479.1_{87}

[a] As a comparison, the same contributions are reported for the external complex formed with the La^{3+} cation. The number -5.4_{15} means -5.4 ± 15.

The Lennard-Jones potential is composed of two terms: one term, depending on the separation by $1/r^{12}$, represents the very short-range repulsion and a second term, depending on $-1/r^6$, is used to model the van der Waals interactions based on dipole/dipole, dipole/induced-dipole, and induced-dipole/induced-dipole interactions (Keesom, Debye, and London dispersion energies). These two terms are reported in Table 1 along with the electrostatic contributions between the calixarene and the alcohol. For the inclusion complexes, Table 1 shows that the dispersion interactions are negative and predominant compared to repulsion interactions whereas the electrostatic term remains very weak. It is also shown that the van der Waals interactions follow the same trend as that observed between the number of inserted atoms and the experimental $\Delta_r H°$ values. In the case of the external complex formed with the La^{3+} cation, the calixarene−cation electrostatic interaction energy is strongly negative (Table 1). The energy calculation is consistent with the conclusions drawn from microcalorimetry experiments for these two types of complexes,[6] that is, an inclusion complex for which the association is enthalpy-driven and governed by

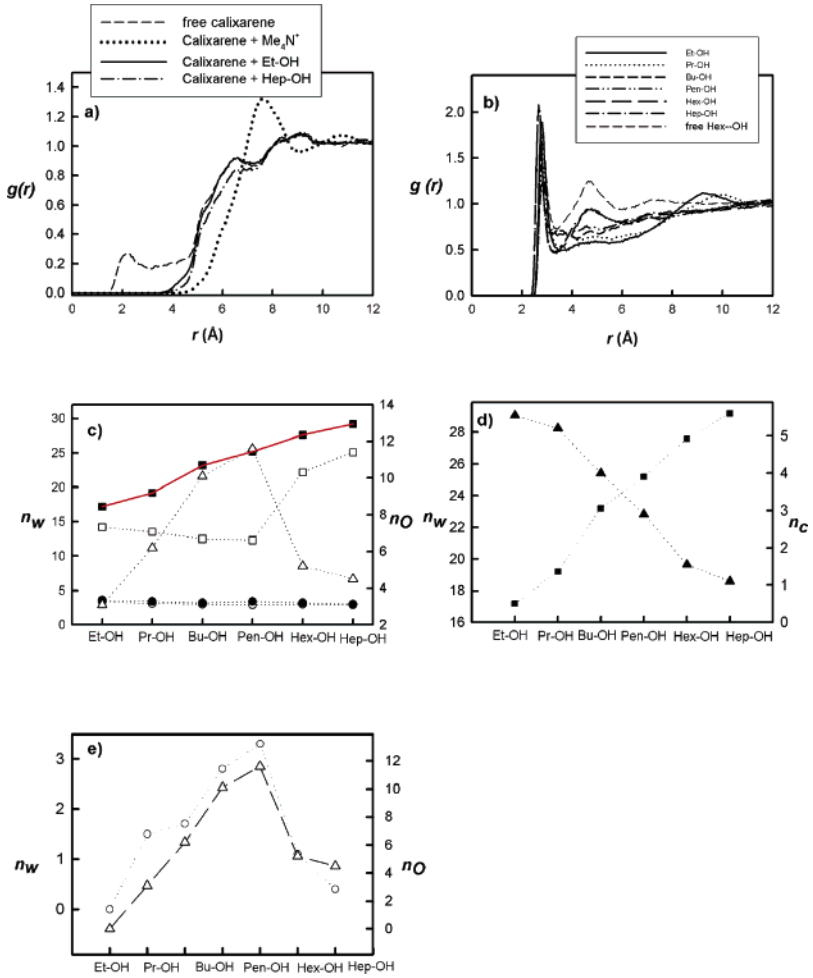

Figure 5. (a) Calixarene com−water O rdf's for different complexes as indicated in the legend; (b) alcohol hydroxy group−water O rdf's; (c) number of water molecules in the first solvation shell of the alcohol OH group in the case of the free alcohol in solution (●) and of the complexed alcohol (○), number of water molecules in the second solvation shell of the alcohol OH group in the case of the free alcohol in solution (■) and of the complexed alcohol (□), number of oxygen atoms of the sulfonate groups in the second solvation shell of the alcohol OH group (△, right axis), and total number of oxygen atoms (water O + sulfonate O) in the second solvation shell of the alcohol OH group (solid red curve); (d) number of water molecules in the first solvation shell of the alcohol OH group for the free alcohol in solution (■, left axis) and number of carbon atoms of the alcohol alkyl chains in the second solvation shell of the hydroxy group (▲, right axis); (e) number of oxygen atoms of the sulfonate groups in the second solvation shell of the alcohol OH group (△, right axis) and number of hydrogen bond bridges between SO_3^- groups and alcohol (○, left axis).

the van der Waals interactions associated with the insertion of alkyl groups and an external complex for which the association process is entropy-driven and controlled by predominant electrostatic interactions.

3.1.2. Desolvation of the Host and Guest. The solvation of the cavity of **1** can be evaluated throughout the calculation of the calixarene com−water O radial distribution function (rdf). We have represented this function in Figure 5a for the complexes with Et-OH and Hep-OH and for the free calixarene in solution. For comparison, we have reported the same rdf for the complex involving the Me_4N^+ cation. The integration of this rdf to the value of the radius of gyration of the macrocycle yields the number of water molecules in the calixarene cavity. This number varies from 4.6 to 5.7 for alcohols whereas it is equal to 8.3 for the free ligand and 0 for the tetraalkylammonium cations. The solvation number and the shape of the rdf show that the desolvation of the calixarene cavity is only partial in the case of alcohols whereas it is total for the tetraalkylammonium cations.

To further investigate the influence of the hydroxy group, we calculate the water O−alcohol OH rdf's in the complexes. These distributions are displayed in part b of Figure 5 and show that the position of the first peak does not depend on the length of the alkyl chain and that it is close to that of the free alcohol in solution. Furthermore, the integration of the first peak of these rdf's shows that the number of water molecules in the first solvation layer of the hydroxy group of the alcohol molecule is the same for the complexed alcohol and the free alcohol, as can be seen in part c of Figure 5. In contrast, the second solvation shell of the complexed alcohol is very perturbed compared to that of the free alcohol. In fact, we observe an evolution of the shape of this part of the curve as a function of the chain length. The peak distinguishing the second solvation shell of the alcohol in the complex is very small from Et-OH to Pen-OH whereas it is much more pronounced and close to that of the free alcohol from Hex-OH. As expected from the rdf's, we check in Figure 5c that the number of water molecules in the second solvation shell of the alcohol OH group is very different in the complex and in the free alcohol. When the peak of the second hydration shell of the alcohol in the complex is not very pronounced, the integration of this peak is carried out using the limit values of r determined in the case of the corresponding free alcohol in water.

Additionally, we show that the evolution of the solvation number of the second solvation layer as a function of the alkyl chain is radically different for the free and the complexed alcohol. We give a microscopic interpretation of the two curves of Figure 5c with respect to the length of the alkyl chain. First, we observe a linear increase of the solvation number of the second shell around the OH group of the free alcohol as a function of the number of carbon atoms of the alkyl chains. We explain this result by calculating the number of carbon atoms in the second solvation shell of the alcohol. We find in Figure 5d a correlation between this solvation number and the number of carbon atoms in this layer. We show that the number of carbon atoms in the second solvation layer decreases as the alkyl chain length increases. The decrease of the hydrophobic matter in the second solvation shell around the alcohol OH group makes the number of water molecules in this layer higher. In the complex, the solvation number of the second shell slightly decreases from Et-OH to Pen-OH with a marked change for Hex-OH and Hep-OH. To understand this behavior, we plot in Figure 5c the number of oxygen atoms of the sulfonate groups located in the second solvation shell of the OH group of the alcohol. The total number of oxygen atoms corresponding to the oxygen atoms of both the SO_3^- groups and water molecules is represented by the solid red line in Figure 5c and matches very well with the number of water oxygen atoms of the second solvation shell of the free alcohol. This means that the oxygen atoms of the SO_3^- groups replace the oxygen atoms of the water molecules in the second solvation shell and allow reconstitution of the second solvation layer with an appropriate coordination number. We see in Figure 5c that the compensation is maximum for Pen-OH with a total of 12 oxygen atoms provided by the SO_3^- groups. Moreover, Figure 5c shows that the complexed Hex-OH and Hep-OH tend to recover the same solvation numbers as those of the free alcohols in water. This result can be explained by the increase of the alkyl chain length which implies that the alcohol OH group moves away from the sulfonate groups. In this case, the second solvation shell around the hydroxy group is mainly constituted of water molecules.

3.1.3. Formation of Hydrogen Bond Bridges. To complete this analysis, we show in Figure 5e the number of hydrogen bond bridges through water molecules that connect the oxygen atoms of the sulfonate groups and the hydroxy group of the alcohol molecule. These particular water molecules belong both to the first solvation shell of the SO_3^- groups and to the second solvation shell of the OH group. The distance criteria for the determination of hydrogen bonds are the same as those used in our previous works.[9,10] To energetically characterize the hydrogen bond bridges, we have calculated the energy contribution between a SO_3^- group and the water molecules of its first solvation shell in different systems. This contribution is equal to -131 ± 6 kJ mol^{-1} for the free calixarene in water. For the complexes with alcohol molecules, it is equal to -139 ± 4 kJ mol^{-1} for water molecules that do not participate to hydrogen bond bridges and varies, depending on the alcohol, from -240 ± 6 to -270 ± 3 kJ mol^{-1} for water molecules involved in hydrogen bond bridges. This result shows the importance of the solvation of the host and guest and the favorable effect of the hydrogen bonding at the enthalpic level.

Figure 6 shows the integration of the distribution of the distance from the hydroxy group of the alcohol and the com of each of the four SO_3^- groups for Et-OH and Hep-OH molecules, respectively. Figure 6a exhibits four similar distributions, indicating that the OH group of Et-OH is located in such a way that the distances with the SO_3^- groups are close together. For

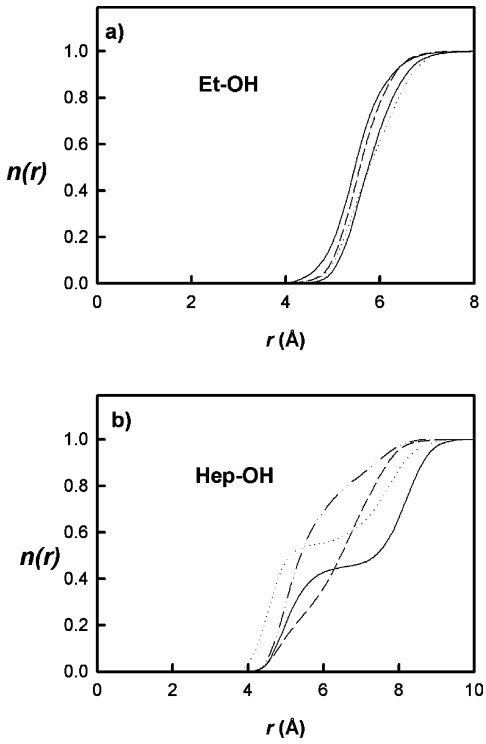

Figure 6. Integrations of the distributions of the distance from each sulfonate group com to the hydroxy group of the alcohol for the complexes with (a) Et-OH and (b) Hep-OH.

Et-OH, the OH group can be considered as inserted into the cavity leading to a loss of degrees of freedom. As concerns the Hep-OH molecule, we observe two integration curves with a flattening in the middle and two other curves with any plateau. The flattenings occur at about 55% and 45%. The presence of zero slope portions indicates that the OH group samples two privileged positions with respect to the diametrically opposed SO_3^- groups. Actually, the fact that, for Hep-OH, the OH group is located above the sulfonate groups and that the number of hydrogen bond bridges is decreased give further degrees of freedom to the hydroxy group.

3.2. Why is Methanol Not Complexed by the Calixarene? In our microcalorimetric study,[6] no heat effect was detected with Me-OH, suggesting that this guest is not complexed by **1**. However, this does not constitute definitive evidence since purely entropic bindings, although scarce, do exist. To check that, we have performed molecular simulation of **1** in the presence of Me-OH.

We have used various starting configurations for the system, but in all cases, we have not observed any association of Me-OH with **1**. This result is important, but it does not allow an explanation for the nonassociation at the enthalpic level. To give a better interpretation of this process, we have thus performed an additional simulation in which the distance between the com of Me-OH and the com of **1** is constrained to 1.5 Å during the simulation. Using this value of distance, we modeled an inclusion complex. The Me-OH molecule is thus inserted into the calixarene cavity with the hydroxy group pointing toward the upper rim of the macrocycle. The average energy contribution between the host and guest for a distance of 1.5 Å is -2.4 ± 0.4 kJ mol^{-1}. Figure 7 shows the methanol OH−water O rdf's calculated in the cases of free methanol in water and inserted methanol into the cavity. When Me-OH is constrained into the calixarene cavity, we observe that the first solvation shell of the alcohol disappears. Let us recall that the first solvation shell of the free Me-OH is composed of three water

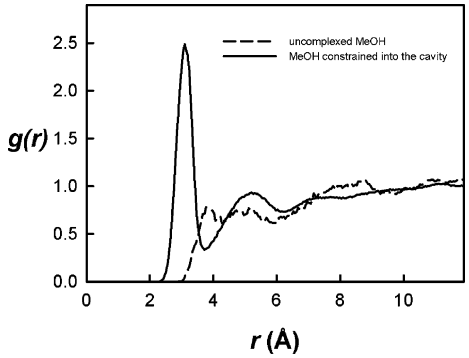

Figure 7. Methanol OH group−water O rdf's in two different cases.

molecules and leads to a favorable energy contribution methanol OH group−water of -241 ± 6 kJ mol^{-1}.

The second solvation shell of the inserted methanol loses 20 water molecules and therefore -19 kJ mol^{-1}. These results show that the favorable energy Me-OH−calixarene contribution (-2.4 kJ mol^{-1}) in the case of a hypothetical complexation is not large enough to compensate the unfavorable desolvation ($(241 + 19)$ kJ mol^{-1}) of the first and second solvation shell of the Me-OH molecule. This result is in agreement with the microcalorimetry experiments.[6]

3.3. Binding with Diols. This section is devoted to the molecular simulations of 1,4-butanediol (OH-Bu-OH) and 1,5-pentanediol (OH-Pen-OH). The microcalorimetric measurements[6] showed that $\Delta_r H°$ and $T\Delta_r S°$ for the binding of Pen-OH are approximately the same as those for the binding of OH-Pen-OH whereas there are important additional positive contributions to $\Delta_r H°$ and $T\Delta_r S°$ when changing from Bu-OH to OH-Bu-OH.

In parts a and b of Figure 8, we show the integrations of the distance from each OH group of OH-Bu-OH and OH-Pen-OH to com$_{OH}$. The comparison with the same distributions calculated in complexes involving Bu-OH and Pen-OH underlines that the hydroxy groups of the diols are much more inserted into the calixarene cavity than the OH group of the corresponding alcohol. In fact, for OH-Bu-OH, at the limit size of the cavity characterized by the distance d_2 (7.5 Å), the two hydroxy groups can be considered as totally inserted into the cavity with percentages of insertion equal to 100% and 94% whereas the insertion rate decreases to 31% for Bu-OH. These percentages of insertion are only equal to 63% and 72% for OH-Pen-OH and 15% for Pen-OH. These results also show that the insertion of the hydroxy groups of the diols is deeper for shorter alkyl chains, as already observed with the alcohols. Furthermore, one of the two integration curves of OH-Bu-OH is shifted to larger distance suggesting that one hydroxy group is more deeply inserted into the cavity. In OH-Pen-OH, each curve presents a first flattening at 50% corresponding to a distance of 6.5 Å and a second flattening at 100 for a distance of 9.0 Å. The fact that the two curves of OH-Pen-OH are similar and present flattenings located at the same distance means that the two hydroxy groups alternatively sample the two same privileged positions, leading to a rocking motion of this diol upon complexation.

Table 2 shows that the average distance between the calixarene com and diol com is really reduced with OH-Bu-OH indicating that the butyl chain is more deeply inserted than the pentyl chain. The maximum insertion rate for OH-Bu-OH is almost reached and should lead to a more favorable value of $\Delta_r H°$ than that determined by microcalorimetry if we take the same line as that followed for the linear alcohols. This is not the case. To further analyze this process, we report in Table 2 the number of water molecules in the first and second solvation shell of each of the two OH groups of the diol with the corresponding OH groups−water molecules energy contributions in the cases of free and complexed diols. In the case of

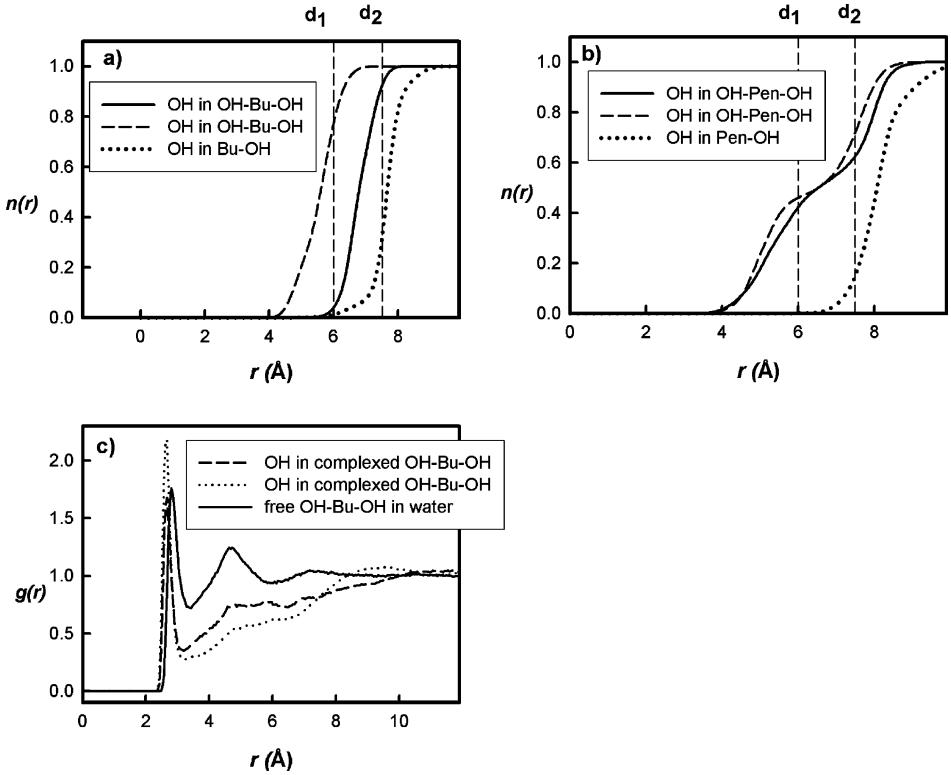

Figure 8. Integrations of the distribution of the distance from the hydroxy groups of the diol to the com$_{OH}$ for complexes involving (a) OH−Bu-OH and (b) OH−Pen-OH diols. As a comparison, the same integration curves are given for the hydroxy groups of Bu-OH (a) and Pen-OH (b) and (c) the diol OH group−water O rdf's.

TABLE 2: Enthalpies (kJ mol^{-1}) and Entropies (kJ mol^{-1}) of Binding of OH-Pen-OH and OH-Bu-OH by 1 in Water at 25 °C[6] and the Average Distance $d_{com..com}$ (Å) Between the Host and Guest and Number $N_{inserted}$ of Atoms Inserted Into the Calixarene Cavity[a]

	OH−Pe*n*-OH ^{free}		OH−Pe*n*-OH ^{bound}		OH−Bu-OH ^{free}		OH−Bu-OH ^{bound}	
$\Delta_r H^o$			-19.3				-4.4	
$T\Delta_r S^o$			-11.1				-2.8	
$d_{com..com}$			5.2_{13}				2.9_3	
$N_{inserted}$			14.6				15.7	
	OH_1	**OH_2**	**OH_1**	**OH_2**	**OH_1**	**OH_2**	**OH_1**	**OH_2**
$N(H_2O)_1$	3.1	3.3	3.1	3.5	3.2	3.0	3.1	1.2
$E(OH-H_2O)_1$	-240_6	-235_5	-244_6	-242_7	-239_5	-238_5	-243_5	-108_4
$N(H_2O)_2$	26.2	26.8	12.3	12.6	24.2	23.8	14.8	8.6
$E(OH-H_2O)_2$	-22_1	-23_1	-7_1	-7_1	-20_1	-20_1	-7_1	-5_1

[a] The superscripts free and bound correspond to the free diol in solution and to the complexed diol. $N(H_2O)_1$ and $N(H_2O)_2$ are the number of water molecules in the first and second solvation shell of each of the two OH groups of the diol, respectively. $E(OH-H_2O)_1$ and $E(OH-H_2O)_2$ correspond to each diol OH group−water molecules energy contributions for the first and second solvation shell around each OH group of the diol. The number -244_6 means -244 ± 6.

OH-Pen-OH, we observe that the first solvation shell around each OH group is not perturbed upon complexation whereas each second solvation shell loses 13 water molecules. We see an identical behavior for each of the two hydroxy groups of OH-Pen-OH. In contrast, for OH-Bu-OH, the surroundings of each of the two OH groups are different. We show in Figure 8c that the diol OH groups−water O rdf's shapes are different for the two hydroxy groups of OH-Bu-OH. In fact, the first solvation shell of one of the two OH groups is changed upon complexation with a loss of two water molecules whereas the second solvation shell of this same hydroxy group is much more desolvated than that of the other OH group with a loss of six additional water molecules. The partial desolvation of the first solvation shell of one of the two OH groups and the increase of the partial desolvation of its second shell lead to additional positive enthalpic contributions, as shown by the energy contributions listed in Table 2. These results are consistent with the conclusions drawn from the microcalorimetric titrations:[6] the fact that the enthalpy and entropy of complexation increases when going from OH-Bu-OH to OH-Pen-OH can indeed be explained by the more important desolvation of one of the two hydroxy groups of OH-Bu-OH. The fact that the $\Delta_r H°$ and $T\Delta_r S°$ values for the binding of Pen-OH are approximately the same as those for OH-Pen-OH, whereas in the diol a second OH group is partially desolvated, implies that an additional negative enthalpic contribution compensates the positive enthalpic cost of this desolvation. This favorable enthalpic contribution can be attributed to the number of hydrogen bond bridges which increases from 3.0 to 5.2 when the guest is changed from Pen-OH to OH-Pen-OH. The snapshots of the complexes of **1** with the alcohols and diols are displayed in Figure 2.

4. Conclusions

The present study has provided a view of the energetics and structures of the binding of linear alcohols and diols by *p*-sulfonatocalix[4]arene in water. We have used the molecular dynamics method to show that the complexes formed with linear alcohols involve the insertion of the alkyl chain. The insertion rate of the hydroxy group of the linear alcohol depends on the alkyl chain length. The MD simulations have highligted a correlation between the experimental $\Delta_r H°$ values and the number of atoms inserted into the cavity of the calixarene. We have shown that the complexes with the alcohols are controlled by van der Waals interactions. In fact, the unfavorable energetic contributions due to the partial desolvation of the host and guest upon binding are largely compensated by the favorable energetic contributions due to van der Waals interactions between the host and guest and to water bridging between the hydroxy group of the alcohol and the sulfonate groups of the calixarene.

We have also clearly established that there is no association between methanol and **1** in water. In fact, the cost of the desolvation in the first and second solvation shell of the hydroxy group of Me-OH is too expensive to be compensated by a favorable Me-OH−calixarene energy contribution.

We have also studied the complexes of **1** with 1,4-butanediol and 1,5-pentanediol. We have shown that the hydroxy groups of the diols are much more inserted into the calixarene cavity than the OH group of the corresponding alcohol. We have explained the important positive contributions to the experimental entropy and enthalpy changes when going from Bu-OH to OH-Bu-OH by the partial desolvation of the first solvation shell of one of the two OH groups of the diol. We have underlined typical different energetic and structural behaviors between the hydroxy groups of OH-Pen-OH and those of OH-Bu-OH by calculating their insertion rate and their solvation number in the first and second solvation shells.

Acknowledgment. The authors acknowledge the Institut du Développement et des Ressources en Informatique Scientifique IDRIS (CNRS) for a generous allocation of CPU time on parallel computers.

References and Notes

(1) Sansone, F.; Segura, M.; Ungaro, R. In *Calixarenes 2001*; Asfari, Z., Böhmer, V., Harrowfield, J., Vicens, J., Eds.; Kluwer Academic Publishers: Dordrecht, The Netherlands, 2001; p 496.

(2) Casnati, A.; Sciotto, D.; Arena, G. In *Calixarenes 2001*; Asfari, Z., Böhmer, V., Harrowfield, J., Vicens, J., Eds.; Kluwer Academic Publishers: Dordrecht, The Netherlands, 2001; p 440.

(3) Bonal, C.; Morel, J. P.; Morel-Desrosiers, N. *J. Chem. Soc., Perkin. Trans. 2* **2001**, 1075.

(4) Douteau-Guével, N.; Coleman, A. W.; Morel, J. P.; Morel-Desrosiers, N. *J. Chem. Soc., Perkin. Trans. 2* **1999**, 629.

(5) Douteau-Guével, N.; Perret, F.; Coleman, A. W.; Morel, J. P.; Morel-Desrosiers, N. *J. Chem. Soc., Perkin. Trans. 2* **2002**, 524.

(6) Perret, F.; Morel, J. P.; Morel-Desrosiers, N. *Supramol. Chem.* **2003**, *15*, 199.

(7) Conway, B. E.; In *Comprehensive Treatise of Electrochemistry, Volume 5, Thermodynamic and Transport Properties of Aqueous and Molten Electrolytes*; Conway, B. E., Bockris, J. O'. M.; Yeager, E.; Eds.; Plenum Press: New York, 1983; Chapter 2.

(8) Mendes, A.; Bonal, C.; Morel-Desrosiers, N.; Morel, J. P.; Malfreyt, P. *J. Phys. Chem. B* **2002**, *106*, 4516.

(9) Ghoufi, A.; Morel, J. P.; Morel-Desrosiers, N.; Malfreyt, P. *J. Phys. Chem. B* **2004**, *108*, 5095.

(10) Ghoufi, A.; Morel, J. P.; Morel-Desrosiers, N.; Malfreyt, P. *J. Phys. Chem. B* **2004**, *108*, 11744.

(11) Cornell, W. D.; Cieplak, P.; Bayly, C. I.; Gould, I. R.; Merz, K. M., Jr.; Ferguson, D. M.; Spellemer, D. M.; Fox, T.; Caldwell, J. W.; Kolleman, P. *J. Am. Chem. Soc.* **1995**, *117*, 5179.

(12) Ryckaert, J. P.; Cicotti, G.; Berendsen, H. J. C. *J. Comput. Phys.* **1977**, *23*, 327.
(13) Tobias, D. J.; Klein, M. L. *J. Phys. Chem.* **1996**, *100*, 6637.
(14) Ota, N.; Brünger, A. T. *Theor. Chem. Acc.* **1997**, *98*, 171.
(15) Jörgensen, W. L.; Chandrasekhar, J.; Madura, J. D. *J. Chem. Phys.* **1983**, *79*, 926.
(16) Allen, M. P.; Tildesley, D. J. *Computer Simulation of Liquid*; Clarendon Press: Oxford, U.K., 1989
(17) Smith, E. R. *Proc. R. Soc. London, Ser. A* **1981**, *375*, 475.
(18) Scharff, J. P.; Mahjoubi, M.; Perrin, R. *New J. Chem.* **1991**, *15*, 883.
(19) Arena, G.; Cali, R.; Lombardo, G. G.; Rizzarelli, E.; Sciotto, D.; Ungaro, R.; Casnati, A. *Supramol. Chem.* **1992**, *1*, 19.
(20) Yoshida, I.; Yamamoto, N.; Sagara, F.; Ishii, D.; Ueno, D.; Shinkai, S. *Bull. Chem. Soc. Jpn.* **1992**, *65*, 1012.
(21) Street, W. B.; Tildesley, D. J.; Saville, G. *Mol. Phys.* **1978**, *35*, 369.
(22) Berendsen, H. J. C.; Postma, J. P. M.; van Gunsteren, A.; DiNola, A.; Haak, J. R. *J. Chem. Phys.* **1984**, *81*, 3684.
(23) Breneman, C. P.; Wiberg; K. B. *J. Comput. Chem.* **1990**, *11*, 361.
(24) Schmit, M. W.; Baldridge, K. B.; Boatz, J. A.; Elbert, S. T.; Gordon, M. S.; Jensen, J. J.; Koseki, S.; Matsunaga, N.; Nguyen, K. A.; Su, S.; Windus, T. L.; Dupuis, M.; Montgomery, J. A. *J. Comput. Chem.* **1993**, *65*, 14.
(25) DL–POLY is a parallel molecular dynamics simulation package developed at the Daresbury Laboratory Project for Computer Simulation under the auspices of the EPSRC for the Collaborative Computational Project for Computer Simulation of Condensed Phases (CCP5) and the Advanced Research Computing Group (ARCG) at the Daresbury Laboratory.
(26) McQuarrie, D. A. *Statistical Mechanics*; University Science Books: Sausalito, CA, 2000; p 264.
(27) Lee, S. H.; Rasaiah, J. C. *J. Chem. Phys.* **1994**, *101*, 6964.
(28) Lyubartsev, A. P.; Laasksonen, A. *J. Phys. Chem.* **1996**, *100*, 16410.
(29) Hawlicka, E.; Swiatla-Wojcik, D. *Phys. Chem. Chem. Phys.* **2000**, *2*, 3175.